A General Theory on the Graphical Representation of Antenna-Radiation Fields

KLAUS W. KARK AND ROLAND DILL

Abstract—**A general theory for graphical representation of antenna radiated fields is developed. The application of the method to the special case of a transverse electromagnetic (TEM)-mode-excited biconical antenna is investigated in detail. Electric field lines in the $r-\vartheta$ plane of a spherical coordinate system are presented in a manner such that the same electric flux is always carried between two neighboring field lines. Thus their mutual distance is a criterion for the strength of the local electric field. The differential equations, which govern the displacement of a field point, are derived and solved. The time-dependent evolution of a field-line pattern is examined in detail. The new theory for graphical field representation permits, in an elegant manner, the analysis of the transmission and receiving mechanism of arbitrary antenna configurations. Thus an iterative graphical synthesis procedure could, in the future, be applied for computer-aided design modeling of antenna shapes.**

I. Introduction

FIELD-LINE PATTERNS can be applied to estimate the rate of convergence of mode-matching methods. At first sight it can be determined how closely the given boundary conditions can already be satisfied with the actual chosen number of modes. Field-line patterns, which show the local strength of the antenna field, can also be used to improve the quality of a given antenna. For instance, the noise temperature of a receiving antenna can be decreased by increasing the conductivity of the boundary of the antenna, where the field strength can reach very high values; i.e., where the field-line density is comparatively high.

Classical antenna design seldom uses field-line information since the numerical effort is quite high; the field strength must be computable with high accuracy at every point of space. But effective computer-aided design modeling of antenna shapes applying graphical synthesis procedures will become more and more important in the future since the available computers will become faster and will have larger memory units.

For certain waveguide and antenna configurations, where the integrability condition is met [1], the standard procedure for contour-line plotting of equipotential lines can be applied to obtain field-line patterns [2]. If this is not the case, a more general technique for field-line representations must be applied. For field-line plotting in waveguides a detailed review of hitherto existing methods has been given by Moller and MacPhie [3].

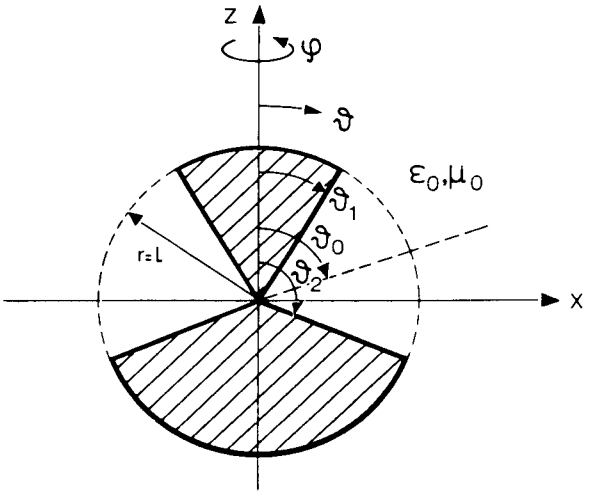

Fig. 1. The biconical antenna: longitudinal section in meridional $r-\vartheta$ plane. ϑ_0 is center angle of the antenna aperture. The spherical surface at $r = l$ defines the junction between the inner and the outer part of the antenna.

We have developed a new general theory on the graphical representation of antenna radiated fields. To demonstrate the behavior of the new technique, a biconical antenna was chosen since its geometrical boundaries can be described as coordinate surfaces of the spherical coordinate system, and the mathematical analysis is therefore rather simple. Transmitting and receiving properties of biconical antennas have been investigated rigorously [4] using mode-matching techniques (orthogonal expansion methods). Rather good approximations for input impedance, directivity, and far-field directional patterns of the transverse electromagnetic (TEM)-mode-excited biconical antenna can even be found, if only a few modes are taken into account for numerical computations [5], [6], [7]. For a graphical near-field representation, however, a more precise field description is necessary.

II. Mathematical Construction of Field-Line Patterns

In this section, the general procedure for the construction of field-line patterns is explained. For mathematical simplicity the special case of a TEM-mode excited biconical antenna (see Fig. 1) is treated, where only two-dimensional electric field lines occur. The described method is nevertheless applicable to three-dimensional field-line patterns of arbitrary antennas as well. The knowledge of the field strength at arbitrary space points is the only presupposition for the application of our method. We calculate the field strength by means of a mode-matching procedure, which is well suited to the considered antenna structure.

Manuscript received February 10, 1988; revised August 4, 1988.

K. W. Kark was with DFVLR Oberfaffenhofen, Institut für Hochfrequenztechnik, Abteilung Hochfrequenzphysik, D-7031 Wessling, West Germany. He is now with the Defense Electronics Division, Siemens AG, P.O. Box 1661, D-8044 Unterschleissheim, West Germany.

R. Dill was with DFVLR Oberpfaffenhofen, Institut für Hochfrequenztechnik, Abteilung Hochfrequenzphysik, D-7031 Wessling, West Germany. He is now with Corporate Research and Development, Siemens AG, Otto-Hahn-Ring 6, D-8000 Munich 83, West Germany.

IEEE Log Number 8931313.

0018-926X/90/0200-0160$01.00

Then the field-line differential equation is derived and numerically solved, and a graphical field representation is finally given. For arbitrary starting points an infinite set of different field lines can be generated. However, for graphical reasons it is more convenient to choose only certain starting points. Assuming that the same electric flux is always carried between two neighboring field lines, a recurrence relation is derived to determine suitable starting points. Thus the distance between two field lines is a criterion for the strength of the local electric field. This way, a general view of the field-strength distribution around the antenna is obtained.

However, the radiation mechanism of an antenna can be analyzed only if the time-dependent behavior of the field-strength distribution is known; i.e., if the displacement of the field lines and their detaching from the antenna is observed. For this purpose a differential equation, which describes the time-dependent movement of a field point, is derived and solved for the first time.

A. Computation of Electromagnetic Fields

The geometrical model of the analyzed biconical antenna is shown in Fig. 1. The arrangement is rotationally symmetrical around the z-axis. The hatched areas are ideally conductive. An ideal source and an ideal sink are concentrated in the origin of a spherical coordinate system. The source excites a TEM-mode whose amplitude is simply chosen to unity, and the sink is a selective absorber used especially for this type of mode. These assumptions simulate the behavior of an ideal antenna feed line, which is prescribed for mathematical simplicity.

In the inner and the outer part of the antenna, lying on opposite sides of the spherical surface at $r = l$, the electromagnetic fields are expanded in infinite eigenfunction series. The expansion coefficients can be determined via an oppositely directed orthogonal expansion. This mode-matching procedure, together with the prescribed expansion direction, guarantees the continuity of the transversal electric and magnetic field strength in the aperture of the antenna at $r = l$.

The exciting TEM-mode has only two field components: E_ϑ and H_φ. Thus, due to the rotational symmetry of the antenna ($\partial/\partial\varphi = 0$), only rotationally symmetrical TM_0-modes are excited. These modes are composed of three field components: E_r, E_ϑ, and H_φ. In the inner antenna region all TM_0-modes are standing waves, since they are reflected at the origin because of the modal selective sink.

B. The Differential Equation of Electric Field Lines

The tangent at an arbitrary point of an electric field line denotes the direction of the electric field vector at this point. This fact can be described mathematically using a line vector element $\vec{ds}$ as follows:

$$\vec{E} \times \vec{ds} = 0. \tag{1}$$

We consider only the $r - \vartheta$ plane of a spherical coordinate system ($\varphi = \text{const.}$). Thus inserting the time-domain electric field vector

$$\vec{E}(t) = E_r(t)\vec{e}_r + E_\vartheta(t)\vec{e}_\vartheta \tag{2}$$

and

$$ds = dr\,e_r + r\,d\vartheta\,e_\vartheta \tag{3}$$

into (1) and normalizing with the propagation constant $k = \omega\sqrt{\mu_0\epsilon_0}$ yields the differential equation for electric field lines:

$$\frac{dkr}{d\vartheta} = kr\frac{E_r(r, \vartheta, t)}{E_\vartheta(r, \vartheta, t)}. \tag{4}$$

This equation is not well suited for numerical evaluations, since there is no one-to-one correspondence between the coordinates r and ϑ along a curve. Hence (4) is transformed to a parameter notation with the infinitesimal arc length ds as a natural parameter [8]. In computing the directional derivatives for the coordinates r and ϑ along a curved field line, one obtains a coupled system of two differential equations:

$$\frac{dkr}{dks} = \frac{E_r}{\sqrt{E_r^2 + E_\vartheta^2}}, \tag{5}$$

$$\frac{d\vartheta}{dks} = \frac{1}{kr}\frac{E_\vartheta}{\sqrt{E_r^2 + E_\vartheta^2}}. \tag{6}$$

Dividing (5) by (6) leads to the original equation, (4). The differential equations (5) and (6) are associated with the following initial values:

$$r(s_0) = r_0, \quad \vartheta(s_0) = \vartheta_0. \tag{7}$$

After selecting a first point of the desired field line (r_0, ϑ_0) or after choosing the corresponding initial parameter s_0, an initial value problem of two ordinary differential equations is obtained. The solution of the differential equation system (5) and (6), and with this the equations of a field line in the $r - \vartheta$ plane, is obtained in an integral representation:

$$kr(s) = kr_0 + \int_{ks_0}^{ks} \frac{E_r(s')}{\sqrt{E_r^2(s') + E_\vartheta^2(s')}}\,dks', \tag{8}$$

$$\vartheta(s) = \vartheta_0 + \int_{ks_0}^{ks} \frac{1}{kr(s')}\frac{E_\vartheta(s')}{\sqrt{E_r^2(s') + E_\vartheta^2(s')}}\,dks'. \tag{9}$$

The field components E_r and E_ϑ are assumed to be known. Using a Runge–Kutta formula of fourth order [9] for systems of differential equations, a consecutive integration of the coupled equations (8) and (9) yields discrete interpolation points along a curved field line. A step size

$$\Delta s = s_{i+1} - s_i \approx \lambda/100 \tag{10}$$

between two neighboring interpolation points s_{i+1} and s_i has proved to be advantageous. λ is the wavelength of the feeding TEM-mode. The computed line points (r_i, ϑ_i) are connected to a continuous field line using a cubic-spline interpolation algorithm.

There is no difference in the procedure for the construction of magnetic field lines. In the considered case of a TEM-mode-excited biconical antenna the magnetic field lines are

concentric circles around the z-axis. Their presentation does not seem to be very interesting and is therefore omitted.

C. Construction of a Field-Line Pattern

Using (8) and (9), it is possible to compute field lines for arbitrary starting points (r_0, ϑ_0). In the following a recurrence relation between the starting points of different field lines is derived. The condition that the same electric flux is always carried between two neighboring field lines must be satisfied. If for all field lines the center angle of the antenna aperture is chosen as starting point ϑ_0

$$\vartheta_0 = \frac{\vartheta_1 + \vartheta_2}{2}, \tag{11}$$

then only the radial distance between two field lines must be considered at ϑ_0. The electric flux Ψ in vacuum, penetrating through an area A, can be described by the following relation:

$$\Psi = \epsilon_0 \int_A \vec{E} \cdot \vec{dA}. \tag{12}$$

If the differential area element is chosen corresponding to

$$\vec{dA} = \sin \vartheta_0 r dr d\varphi \vec{e}_\vartheta, \tag{13}$$

and only the absolute value of E_ϑ is retained, then from (12) following formula can be derived for all rotationally symmetrical TM_0-modes:

$$\Psi = \frac{2\pi\epsilon_0}{k^2} \sin \vartheta_0 \int_{kr_0^\upsilon}^{kr_0^{\upsilon+1}} |E_\vartheta| kr\, dkr. \tag{14}$$

The choice of $\vec{dA}$ as in (13) gives rise to a neglect of the radial electric flux component in the recurrence relation (14). This flux component is produced by an electric field component E_r at the center angle ϑ_0 of the aperture. However, this neglect means no essential restriction, since the relation $E_r(r, \vartheta_0) = 0$ holds for a TEM-mode-fed symmetrical biconical antenna. In addition the nonsymmetrical antenna produces:

$$\frac{|E_r(r, \vartheta_0)|}{|E_\vartheta(r, \vartheta_0)|} \ll 1. \tag{15}$$

The absolute value in (14) assures that oppositely directed fluxes cannot be compensated, if the integration is performed over a zero value of the electric field-strength component E_ϑ. Equation (14) defines the recurrence relation between the starting point r_0^υ of the υth field line and the starting point $r_0^{\upsilon+1}$ of the $(\upsilon + 1)$th field line. After having selected the starting points of the first two field lines r_0^1 and r_0^2 the constant flux Ψ is then defined. The solution of (14) using a Newton iteration leads to the desired value $r_0^{\upsilon+1}$. Thus the starting points r_0^3, r_0^4, $r_0^5, \cdots$ of all other field lines are found. Hence the fixed-point iteration can be written as

$$\frac{\partial \Psi}{\partial \upsilon} = 0. \tag{16}$$

A starting value of

$$kr_0^{\upsilon+1} = 2kr_0^\upsilon - kr_0^{\upsilon-1} \tag{17}$$

for $\upsilon = 2, 3, 4, \cdots$ has proved to give good convergence. The integral in (14) must be solved numerically, even for an analytically given eigenfunction representation of the field components, because of the absolute value of E_ϑ. For accuracy reasons, we preferred the Gauss quadrature technique (see [10]).

Figs. 2(a)–2(c) demonstrate the dependence of the field-line pattern of the biconical antenna on the center angle ϑ_0 of the aperture. For a constant aperture angle $(\vartheta_2 - \vartheta_1 = 40°)$ and the same TEM-excitation, ϑ_0 is chosen as 40°, 65° or 90°. The representation is restricted to the $r - \vartheta$ plane and to the moment $t = t_0$. The initial phase angle ωt_0 is taken for zero. The direction of the field lines has not been indicated. The patterns are mainly rotated toward each other and appear quite similar near the main lobe, but are significantly changed in off-center directions.

In Figs. 2(a) and 2(b) the field distributions for two nonsymmetrical biconical antennas are presented. It is noteworthy that the dimensions of both antennas permit the existence of a special kind of field line, which has already detached from the upper cone, but is still guided by the lower cone. As shown in Fig. 2(a), also inside the biconical antenna some field lines reverse before having reached the opposite conical boundary. These two remarkable phenomena cannot exist in the TEM-mode-excited symmetrical biconical antenna (see Fig. 2(c)).

D. Time-Dependent Variations of a Field-Line Pattern

Figs. 2(a)–2(c) show the field lines of biconical antennas at discrete moments $t = t_0$. In the following the evolution of such field patterns will be investigated for different moments

$$t = t_0 + n\tau \quad \text{with} \quad n = 1, 2, 3, \cdots. \tag{18}$$

τ is a suitable chosen time distance between two neighboring snapshots. We assume that a single point of a field line, which can be identified with an infinitesimal small energy package, propagates with an instantaneous energy velocity $v_E(t)$ [11]. For this field point a differential equation can be derived, which describes its time-dependent displacement. The energy velocity is the derivative of the energy path $\vec{ds}$ with respect to the time. In the $r - \vartheta$ plane the following vector differential equation holds:

$$v_E = \frac{\vec{ds}}{dt} = \frac{dr\vec{e}_r + rd\vartheta \vec{e}_\vartheta}{dt}, \tag{19}$$

which can equivalently be expressed in scalar notation:

$$\sqrt{\mu_0\epsilon_0} v_E \cdot \vec{e}_r = \frac{dkr}{d\omega t}, \tag{20}$$

$$\sqrt{\mu_0\epsilon_0} v_E \cdot \vec{e}_\vartheta = kr \frac{d\vartheta}{d\omega t}. \tag{21}$$

Replacing in both (20) and (21) the energy velocity v_E by the ratio of energy-flux density $\vec{P}$ and energy density w with $Z_0 = \sqrt{\mu_0/\epsilon_0}$ as the characteristic impedance of the free space

$$v_E(t) = \frac{P(t)}{w(t)} = \frac{E \times H}{\frac{\epsilon_0}{2}(E^2 + Z_0^2 H^2)} \tag{22}$$

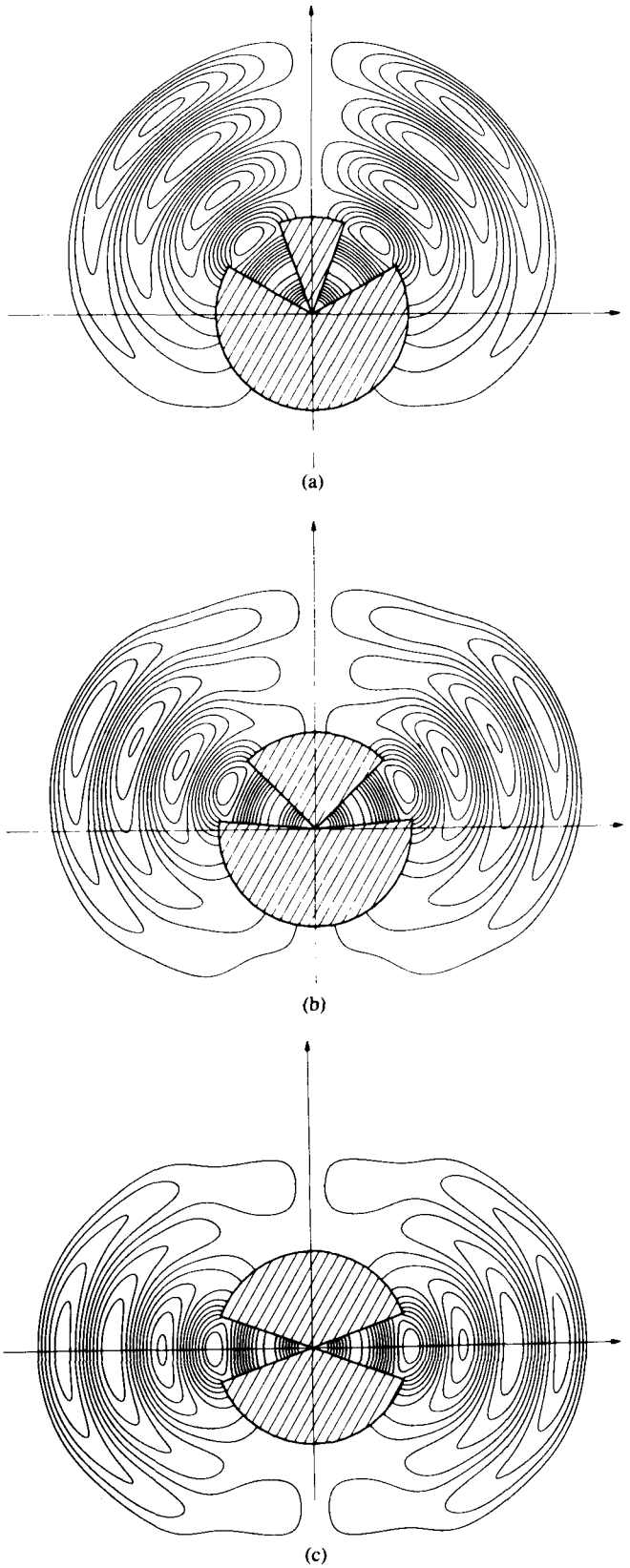

Fig. 2. Electric field lines: field patterns of related biconical antennas at $t = t_0 = 0$ with equal aperture angles. The antennas are fed by a TEM-mode. Geometrical dimensions are: $l/\lambda = 1$ and $\vartheta_2 - \vartheta_1 = 40°$. The different center angles of the aperture are chosen as $\vartheta_0 = 40°$, 65°, 90°.

leads to the following differential equation system for rotationally symmetrical TM_0-modes, which is suited for determining the energy path:

$$\frac{dkr}{d\omega t} = 2\frac{Z_0 E_\vartheta H_\varphi}{E_\vartheta^2 + E_r^2 + (Z_0 H_\varphi)^2}, \tag{23}$$

$$\frac{d\vartheta}{d\omega t} = -\frac{2}{kr}\frac{Z_0 E_r H_\varphi}{E_\vartheta^2 + E_r^2 + (Z_0 H_\varphi)^2}. \tag{24}$$

With the initial values

$$r(t_0) = r_0 \tag{25}$$

and

$$\vartheta(t_0) = \vartheta_0 = \frac{\vartheta_1 + \vartheta_2}{2} \tag{26}$$

the coupled equations for the time-dependent space motion of a point of a field line can be written as follows:

$$kr(t) = kr_0 + 2\int_{\omega t_0}^{\omega t} \frac{Z_0 E_\vartheta(t') H_\vartheta(t')}{E_\vartheta^2(t') + E_r^2(t') + Z_0^2 H_\varphi^2(t')}\, d\omega t', \tag{27}$$

$$\vartheta(t) = \vartheta_0 - \int_{\omega t_0}^{\omega t} \frac{2}{kr(t')} \frac{Z_0 E_r(t') H_\varphi(t')}{E_\vartheta^2(t') + E_r^2(t') + Z_0^2 H_\varphi^2(t')}\, d\omega t'. \tag{28}$$

Equations (27) and (28) are solved for a given moment t analogously to (8) and (9) using a Runge–Kutta formula of fourth order. For the numerical evaluation of the integrals a time-discrete step size Δt has proved to be advantageous:

$$\Delta t \approx T/300, \tag{29}$$

where T represents the time period ($T = 2\pi/\omega$). The computed field-line points are then used as starting points for the complete field-line construction as shown in Section II-B.

Figs. 3(a)–3(d) demonstrate the field-pattern evolution for a nonsymmetrical biconical antenna in the $r - \vartheta$ plane at different moments $t = t_0 + n\tau$ during a half-period $T/2$. The time distance τ between two snapshots is chosen as follows:

$$\tau = T/8. \tag{30}$$

The computing time for a complete field-line pattern at a fixed moment t strongly depends on the aperture angle ($\vartheta_2 - \vartheta_1$) and on the spatial step size Δs. On an IBM 3090 computer a CPU-time of about 50 s is consumed for an aperture angle of order 60° and for a step size $\Delta s \approx \lambda/100$. The longest field lines in Figs. 3(a)–3(d) consist of about 1000 interpolation points.

III. Generalization and Concluding Remarks

The presented new algorithm for graphical representation of electromagnetic fields around antennas requires only the knowledge of the field strength at arbitrary space points and

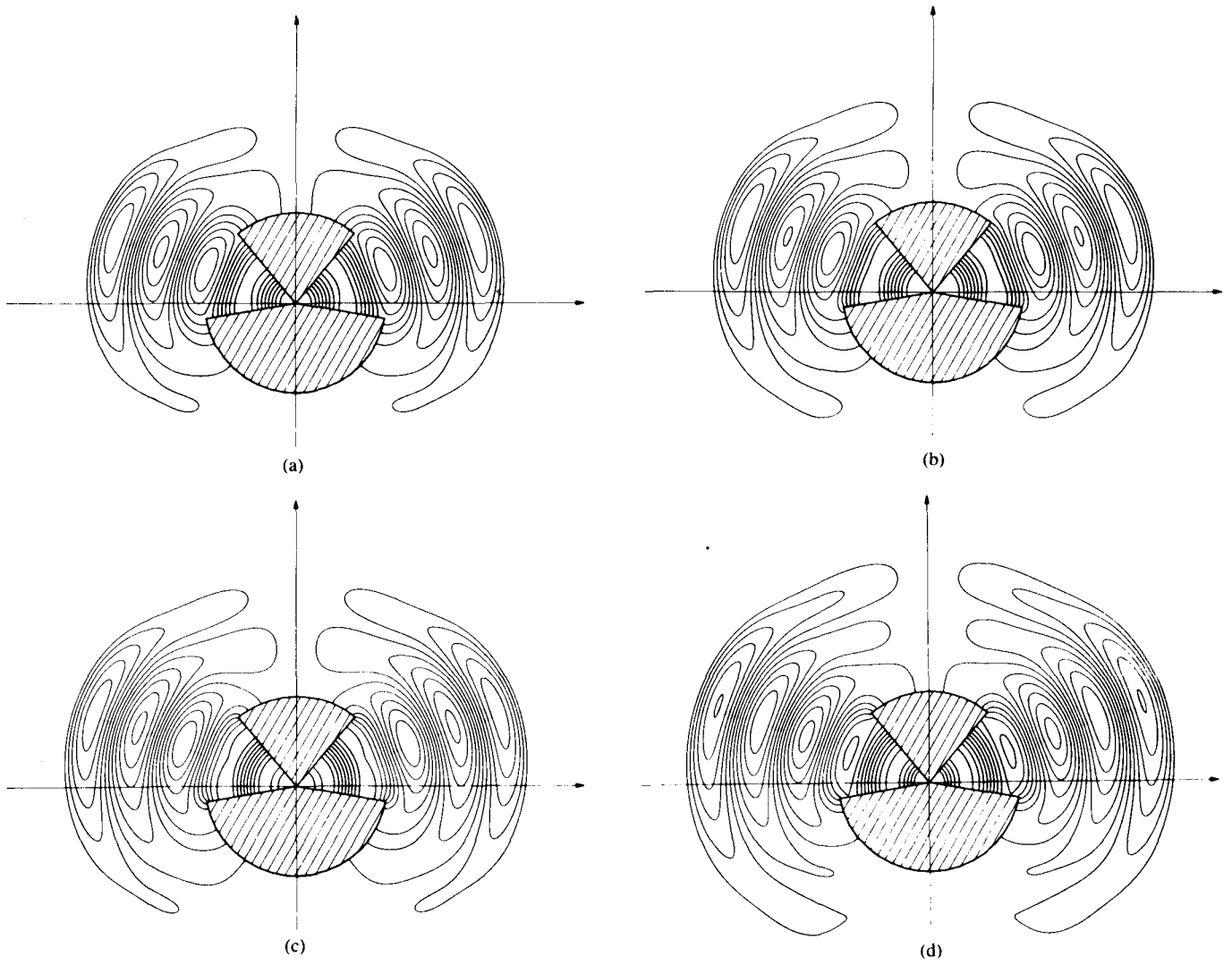

Fig. 3. Field-pattern motion: field patterns of a nonsymmetrical biconical antenna at different moments $t = t_0 + n\tau$ ($t_0 = T/16$, $\tau = T/8$ and $n = 0, 1, 2, 3$). The antenna is fed by a TEM-mode. Dimensions of the antenna are: $l/\lambda = 1$, $\vartheta_1 = 40°$ and $\vartheta_2 = 100°$.

information about the geometrical shape and the location of the considered structure. The described procedure takes into account a physically meaningful field-line density and the time-dependent evolution of the whole field-line pattern. The general ideas, independent of the considered special arrangement, can be summarized as follows:

- numerical solution of the field line differential equation in parameter notation;
- flux computation and choice of field-line starting points;
- computation of the energy-path and the displacement of total field lines.

Although the application of this formal algorithm may be quite different for different types of antenna structures, the overall technique is sufficiently general to apply to any antenna configuration and even to waveguides.

Since the Hertzian dipole can be derived as a geometrical limiting case of the biconical antenna, the field-line patterns of this kind of antenna can also be generated using the existing software package. To obtain additional information about the radiation mechanism it would be worthwhile to investigate, after some minor manipulations with the existing software package, the time-averaged energy flux of the biconical antenna and of the Hertzian dipole. This quantity is of great importance, since its graphical representation can give an intuitive understanding of the directivity of an antenna.

The created Fortran computer program is well suited to produce the snapshots for a film, which demonstrates the radiation behavior of a biconical antenna. First experience indicates that it would be advisable to subdivide a half-period into 64 separate pictures ($\tau = T/128$).

Acknowledgment

The theoretical investigations and the computer programming were carried out during the stay of both authors at the Institute of High Frequency Techniques at the University of Darmstadt, West Germany. The authors sincerely wish to

thank Professor Dr. Anton Vlcek (Darmstadt University) for helpful discussions.

REFERENCES

[1] E. Kamke, *Differential Equations*. Leipzig: Akademische Verlagsgescellschaft, 1967 (in German).
[2] B. Müller, "The computation of the electromagnetic field around a receiving antenna," *AEÜ*, vol. 26, pp. 73–79, 1972.
[3] P. E. Moller, and R. H. MacPhie, "On the graphical representation of electric field lines in waveguide," *IEEE Trans. Microwave Theory Tech.*, vol. MTT-33, pp. 187–192, 1985.
[4] D. M. Grimes, "Biconical receiving antenna," *J. Math. Phys.*, vol. 23, pp. 897–914, 1982.
[5] S. A. Schelkunoff, *Electromagnetic Waves*. New York: Van Nostrand, 1943.
[6] C. H. Papas, and R. King, "Input impedance of a wide-angle conical antenna fed by a coaxial line," *Proc. IRE*, vol. 37, pp. 1269–1271, 1949.
[7] ——, "Radiation from wide-angle conical antennas fed by a coaxial line," *Proc. IRE*, vol. 39, pp. 49–51, 1951.
[8] G. Greving, "A method for numerical computation of three-dimensional field lines," *AEÜ*, vol. 28, pp. 310–313, 1974.
[9] J. Todd, *Survey of Numerical Analysis*. New York: McGraw-Hill, 1962.
[10] M. Abramowitz and I. A. Stegun, *Handbook of Mathematical Functions*. New York: Dover, 1972.
[11] H. Liska, "Energy transport in electromagnetic fields," Dr. Ing. dissertation, Dept. Elec. Eng., Munich Univ., 1970 (in German).

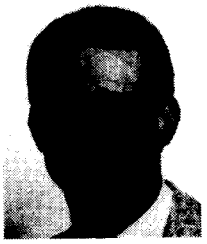

Klaus W. Kark was born in Lampertheim, West Germany, in 1961. He received the Dipl. Ing. degree and the Dr. Ing. degree (summa cum laude) both from the University of Darmstadt, Darmstadt, West Germany, in 1984 and 1987, respectively.

During 1984–1989 he was with the Institute for Radio Frequency Technology at the German Aerospace Research Establishment (DFVLR) in Oberpfaffenhofen. In 1989 he joined Siemes AG, Defense Electronics Division, Munich. His research interests include analytical methods for electromagnetic boundary value problems with emphasis on high-frequency phenomena. He is mainly concerned with microwave antenna and waveguide scattering problems, applying rigorous and perturbational methods and high-frequency approximation techniques. Currently, he is working on the analysis of reflector antennas and waveguide discontinuity problems.

Dr. Kark received the Hugo-Denkmeier Award in 1987.

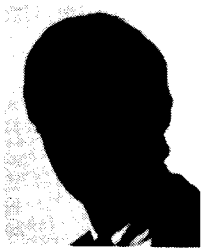

Roland Dill was born in Grossostheim, West Germany, in 1956. He received the Dipl. Ing. degree and the Dr. Ing. degree, both from the University of Darmstadt, Darmstadt, West Germany, in 1982 and 1987, respectively.

In 1982 he joined the Institute of High Frequency Techniques at the University of Darmstadt, where he was engaged in the theoretical and experimental investigation of microwave antennas. He has been working at Siemens, AG, Corporate Research and Development, Munich, since 1987, where he is developing SAW devices and passive HTSC components for analog signal processing.